Formulation of semi-solid dosage forms indented for transdermal delivery of ivermectin

Article *in* Journal of Drug Delivery Science and Technology · November 2024

DOI: 10.1016/j.jddst.2024.106174

4 authors, including:

Hendrik J.R. Lemmer
North-West University
16 PUBLICATIONS **184** CITATIONS

SEE PROFILE

Minja Gerber
North-West University
59 PUBLICATIONS **1,702** CITATIONS

SEE PROFILE

Journal of Drug Delivery Science and Technology 101 (2024) 106174

Contents lists available at ScienceDirect

Journal of Drug Delivery Science and Technology

journal homepage: www.elsevier.com/locate/jddst

Formulation of semi-solid dosage forms indented for transdermal delivery of ivermectin

Zia Aucamp, Wilna Liebenberg, Hendrik J.R. Lemmer, Minja Gerber *

Centre of Excellence for Pharmaceutical Sciences (Pharmacen™), North-West University, Private Bag X6001, Potchefstroom, 2520, South Africa

1. Introduction

The story of ivermectin originated in 1974, when scientist Satoshi Omura discovered *Streptomyces avermitilis*, which later led to the isolation of an active compound, avermectin and finally, ivermectin [1]. Ivermectin, which consists of two homologs (namely dihydro-avermectin B_{1b} and dihydro-avermectin B_{1a}) [2], is a broad-spectrum anti-parasitic drug. It was initially employed in the veterinary field of medicine; however, in 1987 it was brought on by Merck as a treatment regime for onchocerciasis, a disease that effected a great percentage of the population in Africa [3]. Since then, ivermectin has been widely used in the treatment of both topical and systemic diseases, which includes, scabies, rosacea, and other filarial infections [4,5]. Ivermectin stimulates the gamma-aminobutyric acid (GABA)--gated chloride ion channels, commonly found in nematodes, insects, and ticks, which leads to paralysis [1,6]. However, its safety in humans has been established due to its inability to cross the blood brain barrier [1]. Despite ivermectin's use over the past few decades, the coronavirus disease 2019 (COVID-19) pandemic has shed a light on the drug; hence, its reported anti-viral activity against the virus has become an intriguing, yet controversial research topic. The speculated mechanism of action in the treatment of the virus, is due to the inhibition of the viral importin (IMB) α/ β1-mediated nuclear import, resulting in the reduction of viral replication [7,8]. Although this active pharmaceutical ingredient (API) is generally well tolerated, some adverse effects, including gastrointestinal upset and abdominal pain, have been reported with oral dosages [5]. Additionally, there are reports documenting the low bioavailability of the drug [9]. The transdermal drug delivery route offers many advantages over conventional routes; some of which includes, avoidance of hepatic first-pass metabolism to increase bioavailability and avoidance of gastrointestinal upset [10,11]. During this study, the focus was on the transdermal and/or topical delivery of ivermectin. Although transdermal drug delivery has many benefits, there are some drawbacks that should be taken into consideration, i.e., the number of APIs that can be delivered *via* this route is limited [11,12]. Ivermectin is a highly lipophilic drug that presents with physicochemical properties far from the ideal physicochemical properties required for transdermal drug delivery, which is why it is anticipated that it will have difficulties permeating the skin. Therefore, three semi-solid formulations, i.e., emulgel, cream, and ointment were formulated during this study to investigate whether any of the formulations could potentially assist in delivering ivermectin transdermally and/or topically.

2. Materials and methods

2.1. Materials

Ivermectin was obtained from DB Fine chemicals (Sandton, South Africa). The surfactants, Span® 60 and Tween® 80 as well as polyethylene glycol 400 (PEG 400) was obtained from Sigma-Aldrich® (Johannesburg, South Africa). Cetyl alcohol, used as a thickening agent and polyethylene glycol 4000 (PEG 4000) was obtained from Merck chemicals. Sodium hydroxide (NaOH) and orthophosphoric acid used for the preparation of phosphate buffered solution (PBS, pH 7.4) were purchased at Sigma-Aldrich® (Johannesburg, South Africa). Carbopol® Ultrez 20 used in the emulgel as a gelling agent was purchased from Lubrizol (Durban, South Africa). Evening primrose oil (EPO) was obtained from Scatter oils, (Johannesburg, South Africa). Ultrapure (UP) water was used throughout the course of this study, which was obtained from Direct Pure® Ultrapure laboratory water purification system (Merck-Millipore, Midrand, South Africa). During the high-performance liquid chromatographic (HPLC) analysis, chromatography grade acetonitrile, methanol and formic acid was used, which was purchased from Associated Chemical Enterprises (ACE) (Johannesburg, South Africa). During the membrane release and skin diffusion studies, Dow Corning® high vacuum grease, Whatman® filter paper and Parafilm® was obtained from Separations (Randburg, South Africa). The immortalized human keratinocytes (HaCaT) cells were donated from the Faculty of Pharmacy at the University of Lisbon, Portugal. Dulbecco's modified eagle medium (DMEM) was obtained from HyClone™ Separations,

* Corresponding author.
E-mail address: Minja.Gerber@nwu.ac.za (M. Gerber).

https://doi.org/10.1016/j.jddst.2024.106174
Received 30 May 2024; Received in revised form 31 July 2024; Accepted 8 September 2024
Available online 12 September 2024

(Johannesburg, South Africa). 1 % Non-essential amino acids (NEAAs) and 1 % penicillin/streptomycin (pen/strep; 10000 U/mL) was obtained from Lonza, Whitehead Scientific (Pty) Ltd, (Cape Town, South Africa). During the cytotoxic studies, 10 % fetal bovine serum (FBS) from Gibco, Thermo Fisher Scientific, (Johannesburg, South Africa), hygromycin (Sigma-Aldrich®), Trypan Blue solution (0.4 %) from HyClone™, Separations, (Johannesburg, South Africa) and Trypsin-Versene® ethylenediaminetetraacetic acid (EDTA) from Lonza™ Whitehead Scientific (Pty) Ltd (Cape Town, South Africa) was used.

2.2. Methods

2.2.1. HPLC analysis of ivermectin

During this study, an HPLC method was developed and validated for the analysis of ivermectin. The HPLC (Shimadzu Nexera-I LC-2040C 3D) was equipped with a quaternary pump, column heater, photo-diode-array (PDA) detector and autosampler injector mechanism. LabSolutions Rev. A. 10.03 acquisition and analysis software was used to analyze the chromatograms. The temperature of the laboratory remained constant (23 °C) throughout the use of the apparatus. The mobile phase consisted of Phase A (UP water and 0.1 % analytical grade formic acid) and Phase B (methanol and 0.1 % formic acid). The injection volume was set as 5 μL with a run time of 4 min and a flowrate of 0.4 mL/min. The UV-detector was set at a wavelength of 243 mm. The retention time was ±3 min with a total run time of 4 min. An isocratic method consisting of 87 % Phase B and 13 % Phase A was used. The limit of detection (LOD) and limit of quantification (LOQ) for ivermectin was calculated as 0.16 and 0.50 μg/mL, respectively.

2.2.2. Preparation of standard solution

Prior to each analysis a serial dilution was prepared and injected into the HPLC to obtain a linear regression curve. A stock solution was prepared by weighing approximately 25 mg of ivermectin in a 100 mL volumetric flask and filling it up to volume with ethanol (EtOH). Thereafter, a 1000 μL pipette was used to create a serial dilution with ten determined concentrations (250.00, 125.00, 62.50, 31.25, 15.63, 7.81, 3.90, 1.95, 0.98, and 0.49 μg/mL). The samples were filtered with a 0.45 μm polyvinylidene difluoride membrane (PVDF) filter before being injected into the HPLC. A linear regression curve with an $R^2 = 1.00$ was obtained.

2.2.3. Physicochemical properties of ivermectin

2.2.3.1. Solubility of ivermectin in phosphate buffer solution. The water bath (Grant® JB series water bath, Grant Industries, Cambridgeshire, United Kingdom) equipped with a Variomag® magnetic stirring plate (Variomag, Daytona Beach, Florida, United States of America) was set a temperature of ~32 °C (normal skin temperature) [13]. Thereafter, 5 mL of PBS (pH 7.4) was added to each of four labeled test tubes. Three test tubes were oversaturated with ivermectin, while the last test tube was used as a control (contained no ivermectin). The four tubes were placed in a water bath to ensure that they properly dissolved. In addition, a small magnetic stirrer was added to each of the test tubes to ensure continuous stirring. After a 24-h period, 1 mL of each the first three test tubes (containing ivermectin) were filtered with 0.45 μm polyfluoro tetraethylene (PTFE) filter into three 100 mL volumetric flask and filled up to volume with EtOH. The ivermectin solutions were ultrasonicated in an Elma Transonic EL540 ultrasonic bath (Elma Schmidbauer GmbH, Singen (Hohentwiel), Germany) for 5 min to ensure proper dissolution. Finally, 1 mL of each volumetric flask was filtered into marked HPLC vials and analyzed in duplicate. The fourth test tube (control) followed the same method as the other three samples.

2.2.3.2. Solubility of ivermectin in EtOH:PBS (3:7), n-octanol and EPO. The solubility of ivermectin in EtOH:PBS in a ratio of 3:7, *n*-octanol as well as EPO was determined during this study following the same method as used to determine the solubility of ivermectin in PBS (pH 7.4). However, 1 mL of the *n*-octanol solution that contained the saturated ivermectin was diluted with 50 mL of EtOH, while 1 mL of the EPO solution that contained the saturated ivermectin was diluted with 100 mL of EtOH, before being analyzed by HPLC.

2.2.3.3. The octanol-buffer distribution coefficient of ivermectin. Equal volumes (10 mL) of both the *n*-octanol and PBS (pH 7.4) were added in one beaker and stirred on a stirring plate to ensure that the two phases obtained co-saturation. After a 24 h period, the mixture was transferred into a separating funnel to separate the phases. The top (*n*-octanol) and bottom phases (PBS, pH 7.4) were transferred into two separate marked beakers.

A volume 2 mL pre-saturated PBS (pH 7.4) was transferred into each of 3 polytops. Thereafter, a saturated amount of ivermectin was added to each polytop and placed in a preheated (~32 °C) water bath (Grant® JB series water bath, Grant Industries, Cambridgeshire, United Kingdom) with a Variomag® magnetic stirring plate (Variomag, Daytona Beach, Florida, United States of America) to rotate for 45 min. Thereafter, 2 mL pre-saturated *n*-octanol was added to each polytop containing the PBS (pH 7.4) and ivermectin. The polytops were placed in a pre-heated (~32 °C) shaker bath for 2 h, after which each sample was transferred to separate Falcon® tubes for centrifugation for 30 min at 15 557 rcf. A volume of 1 mL of each phase (*n*-octanol and PBS (pH 7.4)) was extracted from each sample and diluted with 100 mL EtOH before it was filtered with 0.45 μm PTFE membrane; thereafter, it was transferred to an HPLC vial, and analyzed by means of the validated HPLC method. Finally, the log D was established by using the concentration ratio of ivermectin in the *n*-octanol and PBS (pH 7.4) phases, respectively. Equation (1) was used to calculate the log D value.

$$\text{Log D} = \frac{\text{Concentration of ivermectin in } n\text{-octanol}}{\text{Concentration of ivermectin in PBS (pH 7.4)}} \qquad \text{Equation 1}$$

2.2.4. Formulation

2.2.4.1. Formulation of emulgel containing ivermectin. Three emulgels containing 2 % ivermectin were formulated containing different ratios of surfactants (Tween® 80 and Span® 60) as well as different concentrations of the gelling agent (Carbopol® Ultrez 20). The oil-phase (Span® 60 and ivermectin) and the water-phase (Carbopol® Ultrez 20, Tween® 80 and UP water) were heated in separate beakers on a magnetic stirring plate to a temperature ~80 °C. Once the temperature was reached, the oil-phase was added to the water-phase in a dropwise manner to create an oil-in-water (o/w) emulsion. The mixture was homogenized at a speed of 13500 rpm for 5 min to ensure proper emulsification. The mixture was left to cool to room temperature (25 °C), after which a few drops of NaOH was added to adapt the pH and create the gel consistency. The selected optimal emulgel was named **EG** (Table 1); in addition, a placebo (no API included) emulgel (named **PEG**) was formulated to serve as a control.

2.2.4.2. Formulation of cream containing ivermectin. Three creams containing 2 % ivermectin were formulated each containing different ratios of surfactants (Tween® 80 and Span® 60) as well as different concentrations of the thickening agent (cetyl alcohol). Span® 60, EPO and cetyl alcohol made up the oil-phase, while the water-phase contained Tween® 80 and UP water. The same method used to formulate the emulgels, was used to formulate the cream. The creams were neutralized to a pH of ±6.0–6.5 with NaOH. The optimal formulation received the name **CR** (Table 1). In addition, a placebo (devoid of API) cream (**PCR**) was formulated to serve as a control.

2.2.4.3. Formulation of ointment containing ivermectin. Three ointments containing 2 % ivermectin were formulated with different ratios of PEG

Table 1
Formulas for semi-solid formulations (50.00 g).

Phase	Excipients	EG (%w/w; g)	CR (%w/w; g)	OM (%w/w; g)
Oil phase	Ivermectin	2.0 % (1.00 g)	2.0 % (1.00 g)	–
	EPO	20.0 % (10.00 g)	20.0 % (10.00 g)	–
	Span® 60	2.0 % (1.00 g)	2.0 % (1.00 g)	–
	Cetyl alcohol	–	10.0 % (5.00 g)	–
Water phase	Carbopol® Ultrez 20	0.4 % (0.20 g)	–	–
	Tween® 80	4.0 % (2.00 g)	3.0 % (1.50 g)	–
	UP water	qs	qs	–
Water soluble base	PEG 400	–	–	56.0 % (27.00 g)
	PEG 4000	–	–	42.0 % (21.00 g)
	Ivermectin	–	–	2.0 % (1.00 g)

400 and PEG 4000. Both excipients were melted in a beaker on a magnetic hot plate, after which ivermectin was added to the beaker. A magnetic stirrer was inserted into the beaker to ensure continuous mixing. After ivermectin completely dissolved, the mixture was left to cool down to room temperature (25 °C), whilst continuous stirring occurred. The selected optimal ointment was named **OM** (Table 1), and a placebo (API absent) ointment (**POM**) was formulated to serve as a control.

2.2.5. Characterization of the semi-solid formulations

2.2.5.1. Visual examination. All the formulations were visually examined on days 1, 3 and 7 following the preparation. This was done to determine if any abnormalities such as, flocculation, sedimentation or aggregation occurred.

2.2.5.2. pH. The pH of the formulation was measured with a Mettler Toledo® pH meter (Mettler Toledo, Columbus, Ohio, United States of America). The pH meter was calibrated prior to each measurement. For the **EG** and the **CR**, the Toledo® InLab® 410 electrode was inserted in the beaker and readings were obtained in triplicate. Due to the high viscosity of the **OM**, 1 g of **OM** was dissolved in 100 mL of UP water before the pH could be measured [14].

2.2.5.3. Droplet size and polydispersity index. The Zetasizer Nano ZS (Malvern® Instruments LTD, Worcestershire, UK) was used to measure the droplet size and polydispersity index (PDI) of the **EG** and **CR**. A drop of each formulation (**EG** and **CR**) was transferred in a 50 mL volumetric flask and filled up to volume with UP water. The solutions were ultrasonicated to ensure proper dissolution. Thereafter, 2 mL was extracted from the solution and transferred to a clear disposable square polystyrene cuvette cell before measurements commenced in triplicate.

2.2.5.4. Zeta-potential. The Zetasizer Nano ZS (Malvern® Instruments LTD, Worcestershire, UK) was used to measure the zeta-potential of the formulations (**EG** and **CR**). The same method used during the determination of the droplet size and PDI was used to prepare samples for zeta-potential. The solution (2 mL) was transferred to a clear capillary zeta-cell. The measurements were taken in triplicate.

2.2.5.5. Viscosity of the formulations. The viscosity of the formulation (**EG** and **CR**) was determined with a Brookfield® Viscometer (model DV II, Stoughton, Massachusetts, USA). Prior to the measurement of the viscosity, the formulations were placed in a thermostatic water-bath connected to the viscometer, allowing it to reach a temperature of ~25 °C. A T-F spindle (Stoughton, MA) was inserted in each formulation. The Helipath stand (D20733) attached to the equipment raised and lowered the rotating spindle. The readings were obtained every 2 min for a period of 10 min, after which the viscosity (cP) was calculated.

2.2.6. Membrane release studies

The membrane release studies were performed on all three formulations (i.e., **EG**, **CR**, **OM**). This was done to determine whether the API was released from the formulation. A PVDF synthetic membrane (Pall® life Sciences, Port Washington, New York, United states of America) was carefully mounted between the donor and the receptor phase of each Franz cell. Dow® corning high vacuum grease was applied to the donor and receptor phases of each Franz cell to allow the two compartments to adhere properly. A small magnetic rod was inserted, which would allow continuous stirring throughout the membrane release studies. The PVDF membrane was carefully placed on the receptor compartment. The two phases were carefully positioned on top of each other, and vacuum grease was applied around the edges of the two phases. The cells were secured with horseshoe clamps to prevent leakage. A volume of 2 mL pre-heated (37 °C) EtOH:PBS (3:7) was transferred to each Franz cell's receptor compartment. The cells were inspected to ensure that no air bubbles were present. A volume of 1 mL of pre-heated (32 °C) formulation (**EG**, **CR** and **OM**) was added to the donor compartment of 10 Franz cells. The remaining 2 cells received the placebos (**PEG**, **PCR** and **OM**). Parafilm® was placed over each Franz cell and plastic caps were placed over to properly cover the donor compartment. The 12 Franz cells were secured in a Franz cell tray and transferred into a pre-heated (~37 °C) water bath (Grant® JB series water bath, Grant Industries, Cambridgeshire, United Kingdom). The study was performed over 6 h with hourly extractions of the content from the receptor phase. Additionally, after each extraction, the receptor compartment was re-filled with 2 mL of fresh PBS (pH 7.4 at 37 °C). The extraction fluid was transferred into marked HPLC vials to be analyzed.

2.2.7. Skin diffusion studies

2.2.7.1. Skin preparation. For this study, donated female Caucasian abdominal skin (ethical approval reference number: NWU-00111-17-A1-19 obtained from The North-West University Health Research Ethics Committee (NWU-HREC)) was used. After informed consent was obtained from the donors, the skin was collected from the surgeons and refrigerated at −20 °C. The skin was prepared by using a Dermatome™ (Zimmer TDS, UK) to cut the skin to a thickness of approximately 400 μm. The dermatomed skin was placed on Whatman® filter paper, wrapped in aluminum foil and kept at −20 °C. Prior to the start of each skin diffusion study, the frozen skin samples were thawed, and inspected for any abnormalities, before being cut into ±15 mm diameter circles. The skin circle was mounted between the two compartments of the Franz cells.

2.2.7.2. Skin diffusion. A similar method used during membrane release studies, was applied during the *in vitro* skin diffusion studies, except that the PVDF membranes were replace with dermatomed skin circles. The skin was mounted between the donor and receptor compartments with the stratum corneum facing upwards. Initially, 2 hourly extractions were taken over 12 h; however, no transdermal data was obtained for any of the formulations; therefore, a single extraction after 12 h occurred.

2.2.8. Tape stripping

Tape stripping was performed after each of the 12-h skin diffusion studies. The two compartments of the Franz cells were carefully disassembled. The skin samples were removed and pinned onto a piece of Parafilm® covering a hard surface. A paper was used to gently dab the

excess formulation on the skin. Approximately 16 pieces of 3M Scotch® Magic™ tape (pre-cut into small pieces) was used to remove the stratum corneum-epidermis (SCE); however, the first strip was discarded to avoid any possible contamination. The remaining strips were added into marked polytops containing 5 mL EtOH (extraction fluid). The glistening skin remaining after the removal of the SCE, which is the epidermis-dermis (ED), was cut into smaller pieces and transferred to marked polytops containing 5 mL of EtOH. All the polytops were refrigerated overnight (12 h). Thereafter, a small quantity of each polytop was extracted, filtered with a 0.45 μm PTFE filter and transferred into marked HPLC vials for analysis, which determined the amount of ivermectin in the SCE and ED, respectively.

2.2.9. In vitro cytotoxicity assay

2.2.9.1. Cell culture cultivation. A significant portion of epidermal cells contain keratinocytes (90–95 %); therefore, the use of human epidermal keratinocytes (HaCaT) can be used to assess the cytotoxicity [15,16]. In addition, one of the three primary cell types in the skin are fibroblasts [17]. BJ-5ta cells (fibroblast cells of human origin) are responsible for collagen production and homeostasis of dermal connective tissues [18]. For this study, the cytotoxicity of ivermectin (**IVM**), the different formulations (**EG**, **CR** and **OM**) and their placebo's (**PEG**, **PCR** and **POM**) were investigated through exposure to HaCaT and BJ-5ta cells.

2.2.9.2. Cell culturing conditions. HaCaT and BJ-5ta cells were preserved in a flask containing high-glucose DMEM. The HaCaT cell line contained added L-glutamine (2.0 mM), 10 % FBS, 1 % NEAA, 1 % pen/strep, while the BJ-5ta cell line also contained Hygromycin® (5 mg/mL). Both flasks were incubated in an ESCO Cell Culture CO_2 incubator (ESCO Technologies, Inc., Missouri, United States America) at 37 °C with a 95 % humidified atmosphere with 5 % CO_2. The cells were inspected every 48 h to check for undesirable bacterial growth. When 80–90 % cell confluency was reached, the cells were treated with trypsin. Trypsinisation is done to ensure the detachment of cells from the primary culture vessel [18], which will allow cells to be transferred to a new vessel where ideal multiplication is possible. Method of exclusion (Trypsin-Versene® ETDA and Trypan blue solution (0.4 %)) was used to establish the concentration of viable cells in the cell suspension. The cell suspension was diluted with growth media to reach a final concentration of 75000 cells/mL for the HaCaT cells and a 60000 cells/mL for the BJ-5ta cells. The HaCaT cells needed to be at a density of 15000 cells per well, whereas the BJ-5ta cells needed to be at a density of 12000 cells per well. Consequently, a multichannel pipette was used to pipette 200 μL of seeding solution into each well. To ensure adequate cell recovery, the cells were then incubated for 24 h. Following the incubation, the cells were treated with different concentrations of **IVM**, **EG**, **CR**, **OM**, **PEG**, **PCR** and **POM**.

2.2.9.3. Methylthiazol tetrazolium (MTT-assay). For the MTT-assays of both HaCaT and BJ-5ta cells, 60 wells per plate were treated. In total, four 96-well plates were used for each cell line. A MTT concentration of 0.5 mg/mL is required for an MTT-assay [19]. After exposure to treatment for 12 h, the plates were removed from the incubator, the treatment solution was aspirated and rinsed with 100 μL of phosphate buffer saline (x2). DMSO wells were filled with 200 μL of pre-heated (37 °C) non-additive DMEM, while the treated, untreated and dead rows received 180 μL of non-additive DMEM. A volume of 20 μL of MTT-solution were added to the rows containing the 180 μL of non-additive DMEM. Before incubating the trays in the CO_2 incubator for 4 h, they were wrapped in aluminum foil since the MTT-solution is light sensitive. The wells were aspirated at the conclusion of the 4-h period, and 200 μL of DMSO was then added to each well to dissolve the crystals that had formed. Once more, aluminum foil covered the plates, and they were shaken for an hour to dissolve the formazan crystals. Each plate was then thoroughly analyzed by the SpectraMax® Paradigm® multi-mode microplate reader (Molecular Devices, San Jose, California, United States of America). The microplate reader was controlled by the SoftMax® Pro 6.2.1 software, and the absorbance was programmed to measure at a cell signal of 560 nm with a background signal of 630 nm.

2.2.9.4. Neutral red (NR) assay. Following the 12 h treatment, the plates were removed from the incubator and all the wells were aspirated. Once again, the rows were rinsed twice with 100 μL of phosphate buffer saline to ensure that no treatment was left on the cells. Non-additive DMEM (200 μL) was added to the solubilization blank wells. A volume of 200 μL of the filtered 10.00 % (v/v) neutral red solution (NRS) was transferred to the treated, untreated, and dead cell control wells. The plates were covered in aluminum foil and incubated for 2 h. After the 2 h incubation period, the wells were aspirated and 100 μL of NR-fixative (1.0 % calcium chloride in 0.5 % formaldehyde) was added to the cells. Immediately thereafter, the wells were aspirated. Lastly, 150 μL of NR-solubilization solution (1 % acetic acid in 50 % ethanol) was added to the wells, the plates were wrapped in aluminum foil and placed in a shaker for 10 min. The same microplate reading used during the MTT-assays was utilized to read the plates; however, the SoftMax® Pro 6.2.1 software allowed the absorbance to be set at 540 nm with a background signal of 690 nm.

2.2.9.5. Data analysis. During the membrane release studies, the average cumulative amount per area released (μg/cm^2) of ivermectin from each formulation was plotted against time [20]. A linear regression curve was obtained, where the slope indicates the average API flux (μg/cm^2.h) [21]. Additionally, the %API released was calculated from the initial concentration incorporated into each formulation. Skin diffusion studies was performed over 12 h, after which the average amount per area diffused (μg/cm^2) after 12 h was calculated. The %API diffused from initial concentration was established. Lastly, an average and median concentration (μg/mL) of ivermectin in the SCE and ED was determined following the analysis of the tape stripping samples.

2.2.10. Statistical data analysis

The membrane release data was analyzed using pair-wise Mann-Whitney U tests with Bonferroni adjustments of the p-values. The tape stripping data compared the SCE and ED with each other for each formulation using a two-way ANOVA. Tukey's honestly significant difference (HSD) test was used as a post-hoc test to determine any statistically significant difference between groups. All membrane release and transdermal statistical analyses were done using Python 3.9 and the Statsmodels library.

3. Results and discussion

3.1. Physicochemical properties of ivermectin

3.1.1. Solubility of ivermectin in PBS, EtOH:PBS (3:7), n-octanol and EPO

The solubility of ivermectin in PBS (pH 7.4) was calculated as 0.013 ± 0.007 mg/mL. Ivermectin's aqueous solubility does not comply with the ideal value (>1.000 mg/mL) required for transdermal drug delivery. Due to the exceptionally low aqueous solubility, EtOH was added to PBS to enhance the sink conditions [22]. The aqueous solubility increased significantly (700 %) upon the addition of 30 % EtOH (EtOH:PBS (3:7)) with a solubility of 0.091 ± 4.839 mg/mL. The solubility in *n*-octanol was determined as 162.778 ± 1.8633 mg/mL, which supported ivermectin's high affinity for the lipophilic phase. The solubility of ivermectin in EPO was 4.971 ± 0.06 mg/mL.

3.1.2. Octanol-buffer distribution coefficient of ivermectin

The octanol-water partition coefficient (log P) and log D can be used

to determine the lipophilicity of compounds [23]. The experimental log D of ivermectin was calculated as 3.69; however, it differed slightly from the reported log P of 3.20 [24]. These experimental differences can be attributed to variations in experimental conditions such as temperature and the use of PBS instead of water [25,26]. Furthermore, a log P between 1.00 and 3.00 indicates that an API possesses both lipophilic as well as hydrophilic properties, these drugs are considered suitable for transdermal drug delivery [10]. Ivermectin's log P (literature) and experimentally determined log D both indicate that it is indeed a lipophilic API.

3.2. Characterization of each drug delivery vehicle

3.2.1. Visual examination

None of the three formulations showed any abnormalities such as flocculation, aggregations, or sedimentation. Both the **EG** and the **CR** presented with a white color and a smooth homogenous texture with the **CR** having an added glossy appearance. The color of the **OM** was slightly opaque, and the texture was homogenous with no presence of lumps.

3.2.2. pH

Table 2 exhibits the pH measurements obtained for all formulations. The **EG**, containing Carbopol® Ultrez 20, was adapted to a pH of approximately 6. This was done to create a desired gel consistency since NaOH reacts with Carbopol® to create a gel network. The **CR** was adapted to reach a pH that correlates with the **EG's** pH. The **OM** obtained a pH of approximately 5. Nevertheless, all three formulations obtained pH values safe for skin application (between 4 and 7) according to Hadgraft [27].

3.2.3. Droplet size and PDI

Table 2 compares the droplet sizes and PDI values of the **EG** and **CR**. The droplet size of an emulsion can give insight to its ability to penetrate the outermost layer of the skin. Droplet sizes smaller than 3 μm will readily penetrate the stratum corneum [28]. Both the **EG** and the **CR** contained values smaller than 3 μm; therefore, theoretically both formulations should be able to penetrate the stratum corneum. Moreover, PDI refers to the polydispersity of a dispersion and its homogeneity [29,30]. A PDI between 0.15 and 0.5 indicates good homogeneity, where a PDI higher than 0.5 and closer to 1.0 indicates an extensive variety between the particle's sizes [31–33]. The **EG** obtained a good PDI, indicating a homogenous distribution of particle sizes. The **CR** obtained a large PDI in comparison to the **EG**; however, it was still considered as an emulsion with homogenous particle size distribution.

3.2.4. Zeta-potential

Zeta-potential speaks to formulation stability and ability to withstand environmental conditions [34,35]. For an emulsion to be classified as stable, the zeta-potential should be higher than +30 mV or lower than −30 mV [36]. Both the **EG** and the **CR** obtained good zeta-potential readings (Table 2), which indicated a high physical stability; however, the **EG** obtained a value considerably higher in comparison to that of the **CR**. The zeta-potential can be affected by droplet size; as droplet size increases, so does the droplet charge, which raises the zeta-potential [37], this statement is proven correct since the **EG** obtained a larger droplet size and a higher zeta-potential measurement in comparison to those of the **CR**.

Table 2
Characterization results of the formulations.

	pH	Viscosity (cP)	Droplet size (r.nm)	PDI	Zeta-potential (mV)
EG	5.997 ± 0.036	28388 ± 209.51	315.5 ± 6.248	0.120 ± 0.093	−51.5 ± 1.307
CR	5.914 ± 0.021	37048 ± 1246.95	119.4 0.625	0.453 ± 0.021	−34.0 ± 0.895
OM	5.007 ± 0.008	–	–	–	–

3.3. Membrane release studies

Table 3 indicates the data obtained during membrane release studies; however, the median flux values were used to discuss the results of the membrane release studies, since it is less effected by outliers than the average [38]. Furthermore, Fig. 1 is included as a visual representation of the data obtained. Upon comparing the median flux value (μg/cm^2.h) for each formulation, it was established that the **OM** obtained the highest median flux, followed by the **EG** and lastly, the **CR**. The **CR** obtained a median flux significantly lower in comparison to the other two formulations. The cetyl alcohol in the **CR** is usually incorporated into topical/transdermal formulations as a structure forming agent, which will create a gel network; subsequently, stabilizing the formulation [39]. The decreased flux seen in the **EG** in comparison to **OM** might be the result of an added gelling agent (Carbopol® Ultrez 20) since the addition of such an excipient tend to decrease the release of an API from the formulation due to its ability to create a film-forming effect [40,41]. Additionally, gel structures inside a vehicle can encapsulate drug particles and further aid in controlled release of an API [42]. Both the **EG** and **CR** contained gelling/thickening agents, explaining the lower flux in comparison to the **OM** that contained no gelling/thickening agents. However, the significantly lower flux of **CR** in comparison to **EG** can possibly be attributed to the quantity of the gelling/thickening agent incorporated into each formulation. The **EG** contained 0.4 % of a gelling agent, while the **CR** contained a much larger concentration of 10.0 %. The **OM** obtained a superlative flux in comparison to the **EG** and the **CR**. This might be attributed to the **OM's** single-phase semi-solid composition [43], where the API is dissolved in PEG 400. Consequently, the API was immediately available for diffusion [44]. The membrane release studies provided insightful information about each formulations' capacity to release the API. Since the API was released from all the formulations, the *in vitro* skin diffusion studies could commence. The one-way Anova revealed that no significant difference existed between the median flux values from the **EG** and **OM** formulations. The post-hoc test revealed that there was statistically significant differences between **EG** and **CR** ($p = 0.0021$) and between **OM** and the **CR** ($p = 0.0021$). The **EG** and the **OM** displayed a membrane release significantly higher ($p < 0.01$) than that obtained from the **CR** (see Fig. 2).

3.4. Skin diffusion

The *in vitro* skin diffusion studies revealed that the **OM** was the only formulation to deliver ivermectin transdermally, obtaining a median amount per area diffused of 0.651 μg/cm^2 (average amount per area diffused of 0.859 ± 0.520 μg/cm^2) after 12 h ($n = 6$). It was speculated that there were various mechanisms that contributed to the successful diffusion of the **OM** through the skin opposed to the **EG** and the **CR**. A recent study on solubility of a lipophilic drug in PEG 400, concluded that higher levels of PEG 400 led to an increased solubility of the drug [45]. Based on this phenomenon, it was speculated that ivermectin might be more solubilized in the PEG 400. Due to the **OM's** possible solubilization capacity, a concentration gradient might have formed, acting as a

Table 3
The average %release (%) together with the average and median flux (μg/cm^2.h) for each formulation after a 6 h membrane release study. The number of Franz cells used is indicated through *n*.

	n	Average %released (%)	Average flux (μg/cm^2.h)	Median flux (μg/cm^2.h)
EG	6	2.510	122.59 ± 21.35	122.82
CR	6	0.020	1.02 ± 0.27	1.01
OM	6	2.341	167.43 ± 42.07	175.03

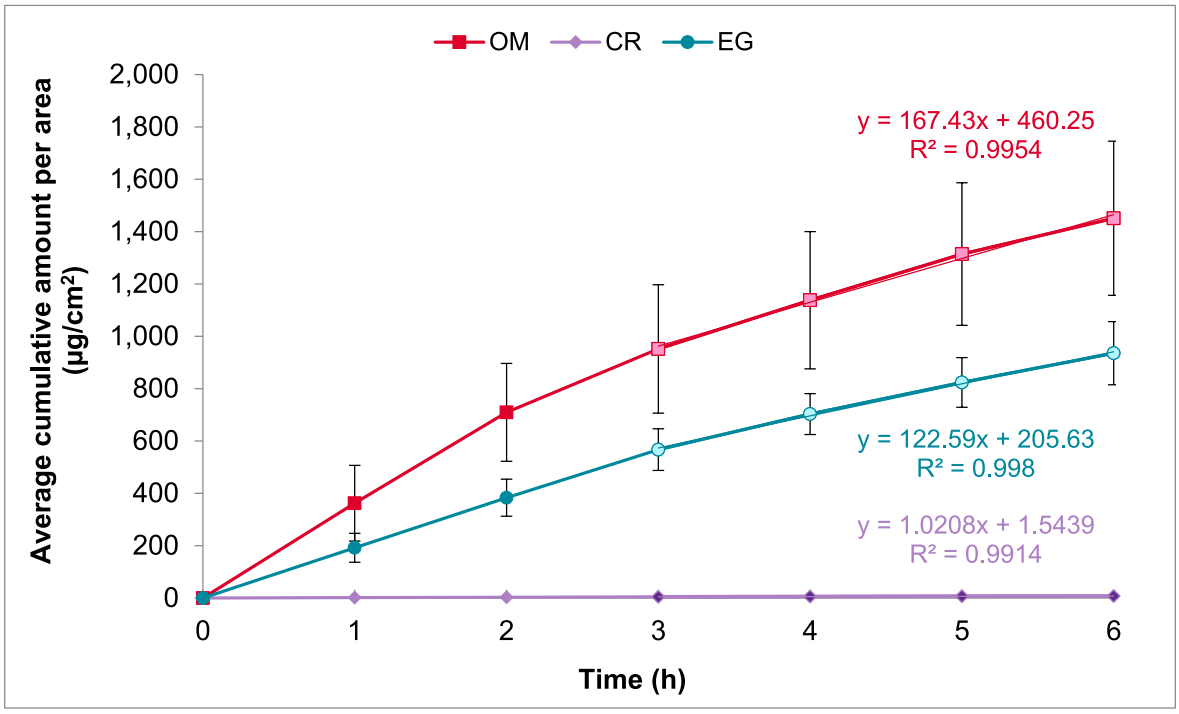

Fig. 1. Average cumulative amount per area released (µg/cm^2) of ivermectin over 6 h during the membrane release studies from all three formulations (**EG**, **CR** and **OM**).

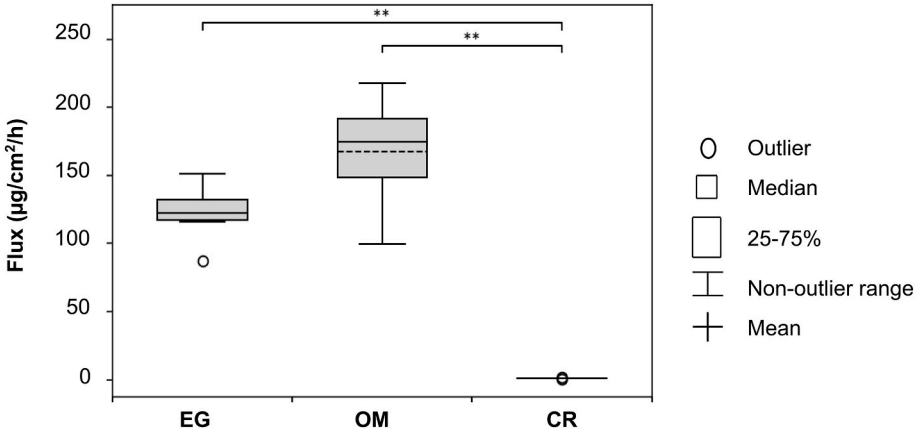

Fig. 2. Boxplot displaying the average and median flux (µg/cm^2/h) of ivermectin from the different formulations (**EG**, **CR** and **OM**) during the membrane release studies over a period of 6 h. The ** indicates statistically significant differences.

driving force for the passive diffusion of ivermectin across the skin layers [46]. Furthermore, a comparison of the structural composition of the **OM**, **EG** and **CR** led to the following observations. The **OM** consisted of a single phase, while the **EG** and the **CR** are both o/w-emulsions, which are classified as multiphase semi-solid formulations [43]. As mentioned before, ivermectin from the **OM** (single phased) will be immediately available for skin diffusion since it avoids partitioning from an aqueous domain to a lipid domain, in contrast to the multiphased semi-solid formulations (**EG** and the **CR**), where drug particles must partition between the oil and water phase, before it can be available for permeation through the skin [44]. Furthermore, the 12 h contact of the **OM** with the skin might have caused hydration of the stratum corneum, which led to swelling and opening of the skin structure, allowing the API to penetrate through the skin [47]. Ointments in general are considered occlusive, which may increase the reservoir volume available to drugs within the stratum corneum, leading to an increased absorption (up to tenfold) according to Ref. [48]. Although, EPO was included in both the **EG** and the **CR** as oil phase and penetration enhancer in attempt to overcome the barrier properties of the skin [49], both formulations were unsuccessful in enhancing the transdermal drug delivery of ivermectin. However, the **OM** contained PEG 400, which has been included in some transdermal formulations as a penetration enhancer [50]. This may have been attributed to further alteration in the barrier properties of the skin.

Upon investigation of the concentration of ivermectin that diffused through the skin and the clinical relevancy of ivermectin, the following was established. Ivermectin is used in the systemic treatment of onchocerciasis; upon the administration of single dose of ivermectin (150 µg/kg), a peak plasma concentration of 40 ng/mL is reached [51]; however, it is difficult to determine whether the concentration ivermectin obtained from the **OM** will produce a therapeutic effect, since skin metabolism influences transdermal drug delivery and *in vitro* studies does not directly correlate to human skin due to the inability of

these studies to mimic exact skin conditions [21].

3.5. Tape stripping

3.5.1. Stratum corneum-epidermis

The median concentration (μg/mL) of ivermectin in the SCE (Table 4), revealed that the API was delivered into the SCE from all three formulations (see Fig. 3). The **EG** obtained the highest median concentration, followed by the **OM** and lastly, the **CR**.

The fatty acids in EPO, acting as chemical penetration enhancers [52], might have contributed to the delivery of ivermectin into the SCE from the **EG** and **CR**. The **CR** and the **EG** contained the same amount of EPO; however, the concentration of ivermectin delivered from the **CR** in the SCE was significantly lower than that of the **EG**. Therefore, it can be concluded that the EPO (acting as penetration enhancer) was not the only mechanism that contributed to the delivery of ivermectin into the SCE. Furthermore, the addition of Carbopol® Ultrez (gelling agent) in the **EG** might have assisted in the higher ivermectin concentration obtained in the SCE for the **EG** in comparison to the **OM** and **CR**, since this gelling agent is known to cause a film-forming effect when applied onto the skin. This film-forming effect might have assisted with the penetration into the SCE [41]. It is important to mention, that the incorporation of gelling agents into a formulation, can increase the API's affinity for the lipophilic SCE [53]. The lipophilic stratum corneum is a formidable barrier that hinders skin penetration [54], but considering that ivermectin is lipophilic in nature (due to its high log P of 3.2 [24], it should be able to penetrate the lipophilic stratum corneum with ease, while the remaining hydrophilic layers of the skin will rather present a barrier to its permeation [47]. With this bore in mind, the ivermectin found in the SCE could be due to the API's lipophilicity and its affinity for the lipophilic barrier rather than the formulations' ability to overcome the barrier properties. The concentration present in the ED for each of the formulations will better reflect on the formulation's role in overcoming the barrier properties of the SCE.

3.5.2. Epidermis-dermis

Upon comparing the median concentration of ivermectin found in the ED (Table 4), it was established that the **OM** delivered the highest concentration of ivermectin into the ED, followed by the **EG**. No ivermectin was found in the ED from the **CR** (**see** Fig. 3).

Despite ivermectin's high lipophilicity, it was observed that the API was not retained in the lipophilic SCE but penetrated through to the hydrophilic ED layer from both the **OM** and the **EG** Ref. [53]; suggesting that the lipophilic matrix barrier was overcome by both formulations (**OM** and **EG**) [55]. Once again, a concentration gradient might have facilitated the permeation from the SCE to the ED due to high concentrations of ivermectin obtained from the **EG** and the **OM** in the SCE (Williams, 2018:718).

To establish therapeutic effectivity of the formulations, the results were compared with Soolantra®, a market product containing 1 % ivermectin, indicated for topically treatment of inflammatory lesion of rosacea [56]. There is uncertainty regarding the pathophysiology of rosacea; however, it might be caused by the overgrowth of the *Demodex* mites, which are natural fauna of the skin, prevalent in the sebaceous glands [57,58]. Literature states that after 1 g of the preparation was applied, the maximum ivermectin plasma concentration of 2.10 ng/mL was reached after 10 ± 8 h [56]. Therefore, a conclusion can be drawn that both the **OM** (0.673 μg/mL in ED) and the **EG** (0.215 μg/mL in ED) might be valuable in the treatment of rosacea. Moreover, it is important to once again mention that the *in vitro* ED results obtained during this study cannot be directly compared to *in vivo* concentrations obtained [21].

Table 4
The average and median concentration (μg/mL) of ivermectin from the different formulations found in the SCE and ED after 12 h. The number of Franz cells used is indicated through *n*.

	n	Average concentration in the SCE (μg/mL)	Median concentration in the SCE (μg/mL)	Average concentration in the ED (μg/mL)	Median concentration in the ED (μg/mL)
EG	9	4.533 ± 2.334	4.537	0.402 ± 0.472	0.215
CR	9	1.437 ± 0.887	1.187	0.000 ± 0.000	0.000
OM	6	3.887 ± 4.264	2.541	0.908 ± 0.449	0.673

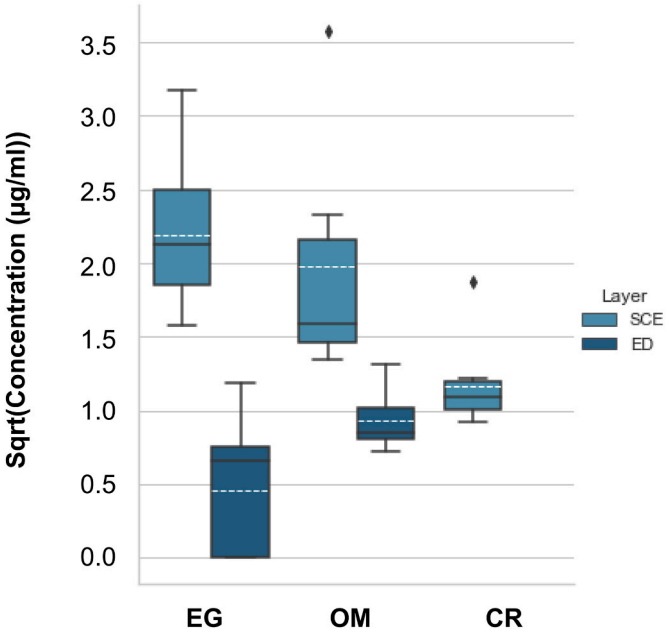

Fig. 3. Boxplot indicating the average and median concentration (μg/mL) of ivermectin from the different formulations (**EG**, **CR** and **OM**) delivered to the SCE and ED after the 12 h skin diffusion study.

A two-way ANOVA was performed to determine statistically significant differences. The post-hoc tests showed that there were statistically significant differences between the concentration of ivermectin present within SCE and the concentration of ivermectin present in ED ($p < 0.05$). Furthermore, statistically significant differences were established between the following groups: **EG** and SCE with **EG** and ED, **EG** and SCE with **OM** and ED, **EG** and SCE with **CR** and SCE, **EG** and SCE with **CR** and ED, **EG** and ED with **OM** and SCE, **OM** and SCE with **OM** and ED, **OM** and SCE with **CR** and SCE, as well as **OM** and SCE with **CR** and ED.

3.6. In vitro cytotoxicity

The untreated control group (with 100 % viability) is used to measure cell viability. By deducting the initial percentage of viable cells from the untreated control group, a regression line was created [59]. Results obtained were presented as a mean ± SD. Figs. 4–5 exhibit the cytotoxicity for the NR- and MTT-assays on both the HaCaT and BJ-5ta cell lines.

3.6.1. MTT-assay

Upon exposure of the treatments (**IVM**, **EG**, **CR** and **PCR**) at the highest concentration (4.00000 μg/mL) to the HaCaT cell line, strong cytotoxicity (%cell viability <40 %) was observed, **PEG** showed moderate cytotoxicity (%cell viability of 40–60 %), while **OM** and **POM** showed weak cytotoxicity (%cell viability of 60–80 %). No cytotoxicity (%cell viability >80 %) was observed for **IVM**, **EG** and **PEG** when HaCaT cells were exposed to a treatment concentration of 0.00315–0.25000 μg/mL, for **CR** at concentrations between 0.00315 and 0.12500 μg/mL, for **OM** at concentrations of 0.00315–0.25000 μg/mL and 1.00000 μg/mL, and for **POM** at concentration of 0.50000 μg/mL and lower. However,

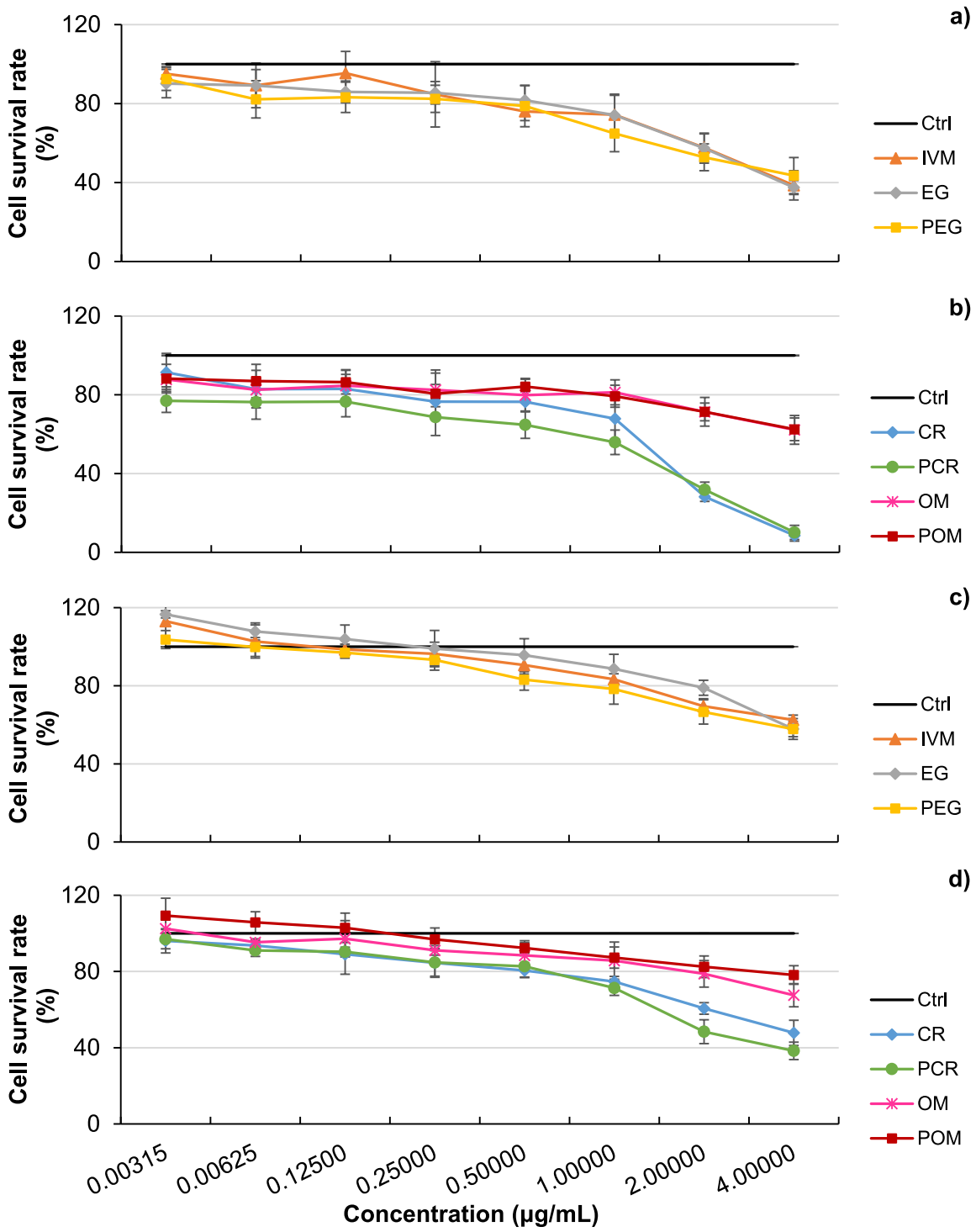

Fig. 4. %Cell viability of HaCaT cells after 12 h exposure to the different concentrations of a) **IVM**, **EG** and **PEG** and b) **CR**, **PCR**, **OM** and **POM** treatments versus the untreated control (Ctrl) during the MTT-assay and c) **IVM**, **EG** and **PEG** and d) **CR**, **PCR**, **OM** and **POM** treatments versus the untreated control (Ctrl) during the NR-assay.

PCR exhibited moderate cytotoxicity at 1.00000 µg/mL and weak cytotoxicity at concentrations of 0.00315–0.50000 µg/mL.

At the highest concentrations (4.00000 µg/mL), the exposure to the BJ-5ta cell line revealed that **IVM** and **EG** were considered weak cytotoxic (%cell viability of 60–80 %), **PEG**, **OM** and **POM** showed moderate cytotoxicity (%cell viability of 40–60 %), while **CR** and **PCR** obtained strong cytotoxicity (%cell viability <40 %). No cytotoxicity (%cell viability >80 %) was observed when **IVM** and **EG** were exposed to concentrations between 0.00315 and 2.00000 µg/mL, when **PEG**, **POM**, **CR** and **PCR** were exposed to concentrations between 0.00315 and 0.50000 µg/mL, and when **OM** was exposed to concentrations between 0.00315 and 0.25000 µg/mL.

3.6.2. NR-assay

The following observations were made regarding the HaCaT cell lines upon exposure to the highest concentration (4.00000 µg/mL): **IVM**,

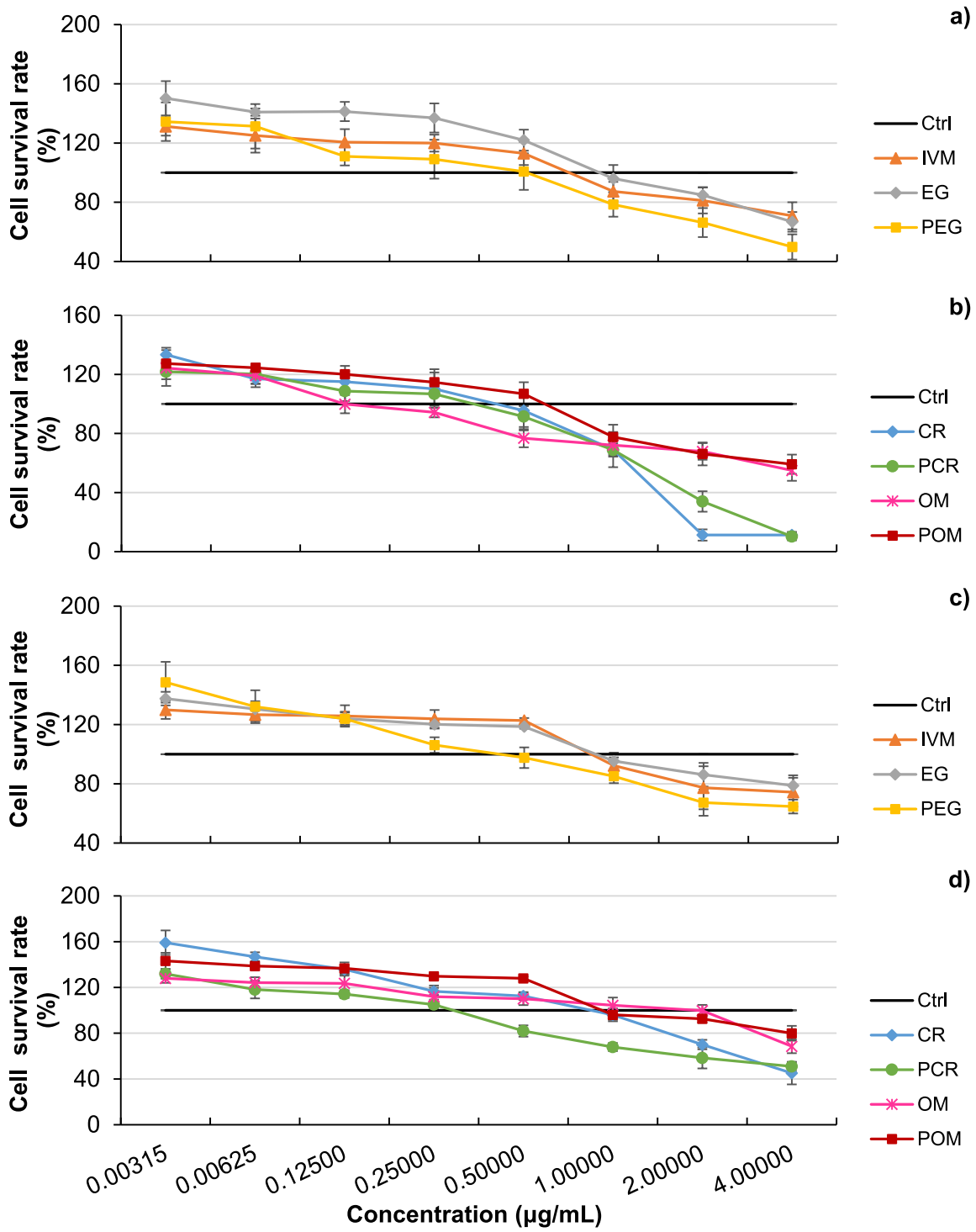

Fig. 5. %Cell viability of BJ-5ta cells after 12 h exposure to the different concentrations of a) **IVM**, **EG** and **PEG** and b) **CR**, **PCR**, **OM** and **POM** treatments versus the untreated control (Ctrl) during the MTT-assay and c) **IVM**, **EG** and **PEG** and d) **CR**, **PCR**, **OM** and **POM** treatments versus the untreated control (Ctrl) during the NR-assay.

OM and **POM** was considered weakly cytotoxic (%cell viability of 60–80 %), **CR**, **EG** and **PEG** was moderately cytotoxic (%cell viability of 40–60 %), while **PCR** was strongly cytotoxic (%cell viability <40 %). No cytotoxicity (%cell viability >80 %) was detected after the HaCaT cells were exposed to **IVM**, **OM** and **POM** at concentrations of 0.00315–1.00000 µg/mL, whilst **CR**, **PCR**, **EG** and **PEG** showed no cytotoxicity at concentrations of 0.00315–0.50000 µg/mL (**EG** also showed no cytotoxicity at 1.00000 µg/mL).

Exposure of the treatments to the BJ-5ta cells led to the following conclusions: **IVM**, **EG**, **PEG**, **OM** and **POM** showed weak cytotoxicity (% cell viability of 60–80 %), while **CR** and **PCR** revealed moderate cytotoxicity (%cell viability of 40–60 %) when exposed to the highest concentrations. No cytotoxicity (%cell viability >80 %) was found for **IVM**, **EG**, **PEG**, and **CR** at concentrations of 1.00000 µg/mL and lower, while **PCR** showed no cytotoxicity at concentrations of 0.50000 µg/mL and lower, whereas no cytotoxicity was observed for both **OM** and **POM** after

exposure to concentrations ranging from 0.00315 to 2.00000 μg/mL.

4. Conclusion

The membrane release studies showed that ivermectin was successfully released from each formulation (**EG**, **CR** and **OM**). Through the *in vitro* skin diffusion and tape stripping studies, it was established that the **OM** was the only formulation to obtain transdermal data, it presented with the highest median concentration in the ED and the second highest median concentration in the SCE. After investigation, a conclusion could be drawn that the structural composition of the **OM** played a great role in its excellent release profile and successful diffusion, since the partitioning phenomenon between phases was avoided and the active was immediately available for skin diffusion. Furthermore, the **EG** presented with the highest median concentration in the SCE and the second highest median concentration in the ED. A concentration gradient formed due to high concentrations in the SCE, which might have acted as a driving force for the passive diffusion of ivermectin from the **EG** into the ED. The **CR** obtained the lowest concentration in the SCE and was absent from the ED. The poor release of the API from the **CR** led to poor delivery of ivermectin in and across the layers of the skin. This proves that API release is an important first step that will affect consecutive steps in the drug permeation of an API across the skin. All three formulations delivered ivermectin into the SCE; however, it might not be solely attributed to the formulation's ability to overcome the formidable barrier but rather the lipophilicity of the API having affinity for the lipophilic stratum corneum. Nevertheless, it was proven that the type of formulation impacts drug delivery in and across the skin [60]. The **CR** and the **EG** were deemed solely as topical preparations while **OM** were successful in delivering ivermectin transdermally. Despite the uncertainty regarding therapeutic effectivity with transdermal concentrations, it was established that the **EG** and the **OM** might be valuable in the treatment of rosacea when compared to plasma levels reached by the market product Soolantra®. To conclude, during the *in vitro* cytotoxic evaluation, it was established that moderate to strong cytotoxicity was observed during both the MTT- and NR-assay on the HaCaT and BJ-5ta cell lines when exposed to the highest concentrations. However, upon investigation of the concentrations equivalent to those found in the ED, weak to no cytotoxicity was observed.

Disclaimer

Any opinions, findings, conclusions or recommendations expressed in this material are those of the authors and therefore the NRF does not accept any liability with regard thereto.

CRediT authorship contribution statement

Zia Aucamp: Methodology, Investigation, Formal analysis, Data curation. **Wilna Liebenberg:** Writing – review & editing, Validation, Supervision, Resources, Project administration. **Hendrik J.R. Lemmer:** Writing – review & editing, Validation, Supervision, Resources, Project administration. **Minja Gerber:** Writing – review & editing, Validation, Supervision, Resources, Project administration, Funding acquisition, Conceptualization.

Declaration of Competing interest

None declared.

Data availability

Data will be made available on request.

Acknowledgements

The authors would like to express their gratitude towards the financial support of the National Research Foundation (NRF) of South Africa: Competitive Programme for Rated Researchers (CPRR) (Grant no. 141957). The authors would also want to thank Prof Frank van der Kooy from the Analytical Technology Laboratory (ATL), Pharmacen™, NWU for his assistance during HPLC method development and validation and Dr Happiness Netshimbupfe, for his guidance during *in vitro* cytotoxic studies in the Mammalian Cell Culture Laboratory in the Laboratory for Analytical and Molecular Biology (LAMB), Pharmacen™, NWU.

References

[1] S. Omura, Ivermectin: 25 years and still going strong, Int. J. Antimicrob. Agents 31 (2) (2008) 91–98, https://doi.org/10.1016/j.ijantimicag.2007.08.023.
[2] L.A. Rolim, F.C.M. Dos Santos, L.L. Chaves, M.L.C.M. Goncalves, J.L. Freitas-Neto, A.L. Da Silva do Nascimento, J.L. Soares-Sobrinho, M.M. De Albuquerque, M. Do Carmo Alves de Lima, P.J. Rolim-Neto, Preformulation study of ivermectin raw material, J. Therm. Anal. Calorim. 120 (1) (2014) 807–816, https://doi.org/10.1007/s10973-014-3691-9.
[3] G.A. Canga, A.M. Prieto, M.J.D. Liébana, N.F. Martínez, M.S. Vega, J.J.G. Vieitez, The pharmacokinetics and interactions of ivermectin in humans—a mini-review, AAPS PharmSciTech 10 (2008) 42–46, https://doi.org/10.1208/s12248-007-9000-9.
[4] E.D. Deeks, Ivermectin: a review in rosacea, Am. J. Clin. Dermatol. 16 (2015) 447–452, https://doi.org/10.1007/s40257-015-0150-8.
[5] D. Rossiter, M. Blockman, K. Barnes (Eds.), South African Medicines Formulary, thirteenth ed., South African Medical Association, Pretoria, 2020.
[6] D. Gupta, A.K. Sahoo, A. Singh, Ivermectin: potential candidate for the treatment of Covid 19, Braz. J. Infect. Dis. 24 (2020) 369–371, https://doi.org/10.1016/j.bjid.2020.06.002.
[7] L. Caly, J.D. Druce, M.G. Catton, D.A. Jans, K.M. Wagstaff, The FDA-approved drug ivermectin inhibits the replication of SARS-CoV-2 *in vitro*, Antivir. Res. 178 (2020) 104787, https://doi.org/10.1016/j.antiviral.2020.104787.
[8] S. Pandey, S.K. Pathak, A. Pandey, A.A. Salunke, J. Chawla, A. Sharma, S. Sharma, P. Thivari, H.V. Ratna, Ivermectin in COVID-19: what do we know? Diabetes Metabol. Syndr. 14 (6) (2020) 1921, https://doi.org/10.1016/j.dsx.2020.09.027.
[9] Z.C. De Souza, F.H.X. Júnior, I.O. Pinheiro, J. de Souza Rebouças, B.O. de Abreu, P. R.R. Mesquita, F. de Medeiros Rodrigues, H.C. Quadros, T.M.F. Mendes, P. Nguewa, S.M. Allegretti, Ameliorating the antiparasitic activity of the multifaceted drug ivermectin through a polymer nanocapsule formulation, Int. J. Pharm. 639 (2023) 122965, https://doi.org/10.1016/j.ijpharm.2023.122965.
[10] D. N'Da, Prodrug strategies for enhancing the percutaneous absorption of drugs, Molecules 19 (12) (2014) 20780–20807, https://doi.org/10.3390/molecules191220780.
[11] D. Ramadon, M.T.C. McCrudden, A.J. Courtenay, R.F. Donnelly, Enhancement strategies for transdermal drug delivery systems: current trends and applications, Drug Delivery and Translational Research (2021) 1–34, https://doi.org/10.1007/s13346-021-00909-6.
[12] M.R. Prausnitz, R. Langer, Transdermal drug delivery, Nat. Biotechnol. 26 (11) (2008) 1261–1268, https://doi.org/10.1038/nbt.1504.
[13] D.G. Wood, M.B. Brown, S.A. Jones, Understanding heat facilitated drug transport across human epidermis, Eur. J. Pharm. Biopharm. 81 (3) (2012) 642–649, https://doi.org/10.1016/j.ejpb.2012.03.019.
[14] A.M. Bhagurkar, M. Angamuthu, H. Patil, R.V. Tiwari, A. Maurya, S. M. Hashemnejad, S. Kundu, S.N. Murthy, M.A. Repka, Development of an ointment formulation using hot-melt extrusion technology, AAPS PharmSciTech 17 (2016) 158–166, https://doi.org/10.1208/s12249-015-0453-3.
[15] S.H. Lee, H.R. Lee, Y.-R. Kim, M.-K. Kim, Toxic response of zinc oxide nanoparticles in human epidermal keratinocyte HaCaT cells, Toxicology and Environmental Health Sciences 4 (1) (2012) 14–18, https://doi.org/10.1007/s13530-012-0112-y.
[16] J. López-García, M. Lehocký, P. Humpolíček, P. Sáha, HaCaT keratinocytes response on antimicrobial atelocollagen substrates: extent of cytotoxicity, cell viability and proliferation, J. Funct. Biomater. 5 (2) (2014) 43–57, https://doi.org/10.3390/jfb5020043.
[17] L. Dong, H. Lee, Z. Liu, D.S. Lee, Anti-skin inflammatory and anti-oxidative effects of the neoflavonoid latifolin isolated from dalbergia odorifera in HaCaT and BJ-5ta cells, Int. J. Mol. Sci. 24 (8) (2023) 7371.
[18] R. Ricardo, K. Phelan, Trypsinizing and subculturing mammalian cells, JoVE (16) (2008), https://doi.org/10.3791/755.
[19] T.L. Riss, R.A. Moravec, A.L. Niles, S. Duellman, H.A. Benink, T.J. Worzella, L. Minor, Cell viability assay, in: Assay Guidance Manual, Eli Lilly & Company and the National Centre for Advancing Translational Sciences, 2016, pp. 1–80.
[20] F. Shakeel, S. Baboota, A. Ahuja, J. Ali, M. Aqil, S. Shafiq, Nanoemulsions as vehicles for transdermal delivery of aceclofenac, AAPS PharmSciTech 8 (4) (2007) 191–199, https://doi.org/10.1208/pt0804104.
[21] S.F. Ng, J.J. Rouse, F.D. Sanderson, V. Meidan, G.M. Eccleston, Validation of a static Franz diffusion cell system for *in vitro* permeation studies, AAPS PharmSciTech 11 (2010) 1432–1441, https://doi.org/10.1208/s12249-010-9522-9.

[22] M. Machado, I.L. Dantas, J.G. Galvão, A.D. Lima, J.K.M. da Cunha Gonsalves, E.D. P. Almeida, G.R.S. de Araujo, L.B. Leal, V.H.V. Sarmento, R.S. Nunes, A.A.M. Lira, Microemulsion systems to enhance the transdermal permeation of ivermectin in dogs: a preliminary *in vitro* study, Res. Vet. Sci. 133 (2020) 31–38, https://doi.org/10.1016/j.rvsc.2020.08.009.
[23] K.D. Freeman-Cook, R.L. Hoffman, T.W. Johnson, Lipophilic efficiency: the most important efficiency metric in medicinal chemistry, Future Med. Chem. 5 (2) (2013) 113–115, https://doi.org/10.4155/fmc.12.208.
[24] M. Liebig, A.A. Fernandez, B. Baum-Gronau, A. Boxall, M. Brinke, G. Carbonell, P. Egeler, K. Fenner, C. Fernandez, G. Fink, J. Garric, B. Halling-Sørensen, T. Knacker, K.A. Krogh, A. Kuster, D. Loffler, M. Angel, P. Cots, L. Pope, C. Prasse, J. Rombke, I. Ronnefahrt, M.K. Schneider, N. Schweitzer, J.V. Tarazona, T. A. Ternes, W. Traunspurger, A. Wehrhan, K. Duis, Environmental risk assessment of ivermectin: a case study, Integrated Environ. Assess. Manag. 6 (1) (2010) 567–587, https://doi.org/10.1002/ieam.96.
[25] l Le Roux, Investigating the transdermal delivery of ketoprofen using different formulation methods, Potchefstroom: NWU. (Dissertation-MSc (2020).
[26] A. Noubigh, A. Mgaidi, M. Abderrabba, Temperature effect on the distribution of some phenolic compounds: an experimental measurement of 1-octanol/water partition coefficients, J. Chem. Eng. Data 55 (1) (2010) 488–491, https://doi.org/10.1021/je900271h.
[27] J. Hadgraft, Skin, the final frontier, Int. J. Pharm. 224 (1–2) (2001) 1–18, https://doi.org/10.1016/s0378-5173(01)00731-1.
[28] B.W. Barry, Drug delivery routes in skin: a novel approach, Adv. Drug Deliv. Rev. 54 (2002) 31–40, https://doi.org/10.1016/s0169-409x(02)00113-8.
[29] S.A. Chime, F.C. Kenechukwu, A.A. Attama, Nanoemulsions- advances in formulation, characterisation, and application in drug delivery, in: A.D. Sezer (Ed.), Application of Nanotechnology in Drug Delivery, InTechOpen, Croatia, 2014, pp. 77–126. https://books.google.co.za/books?hl=en&lr=&id=XiShDwAAQBAJ&oi=fnd&pg=PA77&dq=Chime,+S.A.,+Kenechukwu,+F.C.+%26+Attama,+A.A.+2014.++Nanoemulsions:+advances+in+formulation,+characterisation+and+application+in+drug+delivery.+&ots=_SIWt1KK1C&sig=uTAKgWQjNCBqE4y_sl4GWD8QaSw&redir_esc=y#v=onepage&q=Chime%2C%20S.A.%2C%20Kenechukwu%2C%20F.C.%20%26%20Attama%2C%20A.A.%202014.%20%20Nanoemulsions%3A%20advances%20in%20formulation%2C%20characterisation%20and%20application%20in%20drug%20delivery.&f=false. Date of access: 23 May 2024.
[30] S. Karmakar, Particle size distribution and zeta potential based on dynamic light scattering: techniques to characterize stability and surface charge distribution of charged colloids, Recent Trends in Matererias: Physics and Chemistry (2019) 117–159.
[31] M. Gaumet, A. Vargas, R. Gurny, F. Delie, Nanoparticles for drug delivery: the need for precision in reporting particle size parameters, Eur. J. Pharm. Biopharm. 69 (1) (2008) 1–9, https://doi.org/10.1016/j.ejpb.2007.08.001.
[32] B. Maddiboyina, H. Roy, R.K. Nakkala, S. Gandhi, M. Kavisri, M. Moovendhan, Formulation, Optimization and Characterization of Raloxifene Hydrochloride Loaded PLGA Nanoparticles by Using Taguchi Design for Breast Cancer Application, vol. 102, Chemical Biology & Drug Design, 2023, p. 457:47, https://doi.org/10.1111/cbdd.14222.
[33] S. Surini, A. Leonyza, C.W. Suh, Formulation and *in vitro* penetration study of recombinant human epidermal growth factor-loaded transfersomal emulgel, Adv. Pharmaceut. Bull. 10 (4) (2020) 586, https://doi.org/10.34172/apb.2020.070.
[34] B. Asmawatia, W.A.W. Mustaphaa, S.M. Yusopa, M.Y. Maskata, A.F. Shamsuddinc, Characteristics of cinnamaldehyde nanoemulsion prepared using APV-high pressure homogenizer and ultra turrax, AIP Conf. Proc. 1614 (2014) 244–250, https://doi.org/10.1063/1.4895203.
[35] R.C.D.A. Ribeiro, S.M.D.A.G. Barreto, E.A. Ostrosky, P.A. Rocha-Filho, L. M. Veríssimo, M. Ferrari, Production and characterization of cosmetic nanoemulsions containing Opuntia ficus-indica (L.) Mill extract as moisturizing agent, Molecules 20 (2) (2015) 2492–2509, https://doi.org/10.3390/molecules20022492.
[36] A.M. Eid, H.A. El-Enshasy, R. Aziz, N.A. Elmarzugi, Preparation, characterisation and anti-inflammatory activity of Swietenia macrophylla nanoemulgel, J. Nanomed. Nanotechnol. 5 (2014) 1–10, https://doi.org/10.4172/2157-7439.1000190.
[37] S.A. Onaizi, Effect of oil/water ratio on rheological behavior, droplet size, zeta potential, long-term stability, and acid-induced demulsification of crude oil/water nanoemulsions, J. Petrol. Sci. Eng. 209 (2022) 109857, https://doi.org/10.1016/j.petrol.2021.109857.
[38] C.B. Thompson, Descriptive data analysis, Air Med. J. 28 (2) (2009) 56–59, https://doi.org/10.1016/j.amj.2008.12.001.
[39] M. Kar, Y. Chourasiya, R. Maheshwari, R.K. Tekade, Current developments in excipient science: implication of quantitative selection of each excipient in product development, in: Basic Fundamentals of Drug Delivery, Academic Press, 2019, pp. 29–83.
[40] M. Faustini, B. Louis, P.A. Albouy, M. Kuemmel, D. Grosso, Preparation of sol− gel films by dip-coating in extreme conditions, J. Phys. Chem. C 114 (17) (2010) 7637–7645, https://doi.org/10.1021/jp9114755.
[41] K. Kathe, H. Kathpalia, Film forming systems for topical and transdermal drug delivery, Asian J. Pharm. Sci. 12 (6) (2017) 1–11, https://doi.org/10.1016/j.ajps.2017.07.004.
[42] M. Kumar, A. Sharma, S. Mahmood, A. Thakur, M.A. Mirza, A. Bhatia, Franz diffusion cell and its implication in skin permeation studies, J. Dispersion Sci. Technol. (2023) 1–14, https://doi.org/10.1080/01932691.2023.2188923.
[43] A.C. Williams, Topical and transdermal drug delivery, in: M.E. Aulton, K.M. G. Taylor (Eds.), Aulton's Pharmaceutics: the Design and Manufacturing of Medicines, fifth ed., Elsevier, London, 2018, pp. 715–738.
[44] E. Haltner-Ukomadu, M. Sacha, A. Richter, K. Hussein, Hydrogel increases diclofenac skin permeation and absorption, Biopharm Drug Dispos. 40 (7) (2019) 217–224, https://doi.org/10.1002/bdd.2194.
[45] N. Fine-Shamir, A. Beig, J.M. Miller, A. Dahan, The solubility, permeability and the dose as key factors in formulation development for oral lipophilic drugs: maximizing the bioavailability of carbamazepine with a cosolvent-based formulation, Int. J. Pharm. 582 (2020) 119307, https://doi.org/10.1016/j.ijpharm.2020.119307.
[46] A. Teichmann, S. Heuschkel, U. Jacobi, G. Presse, R.H. Neubert, W. Sterry, J. Lademann, Comparison of stratum corneum penetration and localization of a lipophilic model drug applied in an o/w microemulsion and an amphiphilic cream, Eur. J. Pharm. Biopharm. 67 (3) (2007) 699–706, https://doi.org/10.1016/j.ejpb.2007.04.006.
[47] H.A. Benson, Transdermal drug delivery: penetration enhancement techniques, Curr. Drug Deliv. 2 (1) (2005) 23–33, https://doi.org/10.2174/1567201052772915.
[48] M.R. Prausnitz, P.M. Elias, T.J. Franz, M. Schmuth, J.C. Tsai, G.K. Menon, W. M. Holleran, K.R. Feingold, Skin barrier and transdermal drug delivery, Dermatology 3 (2012) 2065–2073.
[49] L. Van Zyl, J. Du Preez, M. Gerber, J. Du Plessis, J. Viljoen, Essential fatty acids as transdermal penetration enhancers, J. Pharmaceut. Sci. 105 (2016) 188–193, https://doi.org/10.1016/j.xphs.2015.11.032.
[50] Y. Zhang, M.E. Lane, D.J. Moore, An investigation of the influence of PEG 400 and PEG-6-caprylic/capric glycerides on dermal delivery of niacinamide, Polymers 12 (12) (2020) 2907, https://doi.org/10.3390/polym12122907.
[51] C. Chaccour, F. Hammann, N.R. Rabinovich, Ivermectin to reduce malaria transmission I. Pharmacokinetic and pharmacodynamic considerations regarding efficacy and safety, Malar. J. 16 (1) (2017) 1–16, https://doi.org/10.1186/s12936-017-1801-4.
[52] J. Baibhav, G. Singh, A.C. Rana, S. Saini, V. Singla, Emulgel: a comprehensive review of the recent advances in topical drug delivery, Int. Res. J. Pharm. 2 (2011) 66–70.
[53] M.N. Sithole, S. Marais, S.M. Maree, L.H. Du Plessis, J. Du Plessis, M. Gerber, Development and characterisation of nano-emulsions and nano-emulgels for transdermal delivery of statins, Expet Opin. Drug Deliv. 18 (6) (2021) 789–801, https://doi.org/10.1080/17425247.2021.1867533.
[54] J.H. Kim, J.A. Ko, J.T. Kim, D.S. Cha, J.H. Cho, H.J. Park, G.H. Shin, Preparation of a capsaicin-loaded nanoemulsion for improving skin penetration, J. Agric. Food Chem. 62 (3) (2014) 725–732, https://doi.org/10.1021/jf404220n.
[55] V.C. Jhawat, V. Saini, S. Kamboj, N. Maggon, Transdermal drug delivery systems: approaches and advancements in drug absorption through skin, Int. J. Pharmaceut. Sci. Rev. Res. 20 (1) (2013) 47–56. https://globalresearchonline.net/journalcontents/v20-1/10.pdf. (Accessed 23 May 2024). Date of access.
[56] Anon, Soolantra™ [package insert]. Galderma laboratories, L.P., fort worth, TX; desember 2014. http://www.accessdata.fda.gov/drugsatfda_docs/label/2014/206255lbl.pdf, 2023. (Accessed 23 May 2024). Date of access.
[57] D.M. Elston, Demodex mites: facts and controversies, Clin. Dermatol. 28 (5) (2010) 502–504, https://doi.org/10.1016/j.clindermatol.2010.03.006.
[58] M. Schaller, S. Riel, R. Bashur, N. Kurup, H. Schnidar, B. Fehrenbacher, Ivermectin treatment in rosacea: how novel smartphone technology can support monitoring rosacea-associated signs and symptoms, Dermatol. Ther. 35 (11) (2022) 1–7, https://doi.org/10.1111/dth.15869.
[59] J. Weyermann, D. Lochmann, A. Zimmer, A practical note on the use of cytotoxicity assays, Int. J. Pharm. 288 (2) (2005) 369–376, https://doi.org/10.1016/j.ijpharm.2004.09.018.
[60] B. Kim, H.-E. Cho, S.H. Moon, H.-J. Ahn, S. Bae, H.-D. Cho, S. An, Transdermal delivery systems in cosmetics, Biomedical Dermatology 4 (10) (2020) 1–12, https://doi.org/10.1186/s41702-020-0058-7.